# SSM/I GEOPHYSICAL RETRIEVALS AND THEIR IMPACT ON NUMERICAL MODELING

Franklin R. Robertson

Roy W. Spencer

NASA/Marshall Space Flight Center
Huntsville, Alabama 35812

John R. Christy
Atmospheric Science and Remote Sensing Laboratory
University of Alabama in Huntsville
Huntsville, Alabama 35899

## 1. INTRODUCTION

The emergence of space-based remote sensing as a unique tool for observing the earth/atmosphere system has heightened appreciation for the role that the global hydrologic cycle plays in climate dynamics and energetics. This interdependency is manifest primarily in cloud radiative forcing and phase changes of water, two physical mechanisms by which moist thermodynamic processes alter the atmospheric mass distribution and, ultimately, motion fields. Remote sensing from space has enabled observational coverage that supplements data poor regions of the globe, most notably over the oceans. In particular, outgoing longwave radiation (OLR) measurements have long served as a proxy for tropical deep convection, permitting studies which seek to understand links between tropical convective forcing and subsequent atmospheric dynamical response.

Infrared and visible imagery depict largely cloud morphology, giving information on cloud presence and approximate vertical location. Passive microwave measurements are a complementary data source for use in determining bulk cloud microphysical characteristics and water vapor amounts when oceans or other water bodies serve as a background against which the atmosphere is observed. The Special Sensor Microwave/Imager (SSM/I) radiometers flying on DMSP spacecraft will provide a long time series of oceanic wind speed, water vapor, cloud water, and precipitation through the 1990's. Utility of these measurements for validation of numerical models is discussed and initial results are presented.

### 1.1 The SSM/I

The first SSM/I was launched in June 1987 into a sun-synchronous near-polar orbit providing up to twice daily coverage, at 0611 and 1811 local sun time. The swath width

is about 1400 km, which results in 50% coverage twice per day near the equator, increasing to 100% coverage twice per day poleward of about $59^{o}$ latitude. It measures brightness temperatures (TB) at 19.35, 22.235, 37, and 85.5 GHz, at both horizontal and vertical polarizations (except only vertical at 22.235 GHz). The instrument scans along a conical surface with a constant earth incidence angle of $53^{o}$, thus keeping spatial resolution constant and polarization orientation constant throughout the scan. Spatial resolutions vary inversely with frequency, from 15 km at 85.5 GHz to about 70 km at 19.35 GHz. One of the strengths of the SSM/I design is a nearly "direct" calibration design allowing both cold space and warm load observations to be made through the same RF components as the earth observations. This allows calibrated TB to be independent of most instrument temperature variations and component characteristic drifts. Future SSM/I's will be launched on demand as previous DMSP spacecraft elements fail, with in general two operating at any given time.

## 1.2 Passive Microwave Retrievals

Satellite passive microwave measurements allow retrievals of certain geophysical parameters useful for the validation (and possibly initialization) of numerical models. The retrievals depend upon the manner in which certain processes (earth surface and atmospheric characteristics) interact with thermal microwave radiation at certain frequencies and polarizations. Often, more than one method can be used to retrieve a single parameter, due to several radiometer channels having somewhat similar responses to that parameter. Retrievals of several of these parameters can only be accomplished over the ocean. These are total integrated water vapor, near-surface wind speed, cloud water, and liquid precipitation estimates. Over land, ice precipitation estimates and snow cover can also be retrieved (but not ice precipitation over snow cover).

### 1.2.1 water vapor

The retrieval of total integrated water vapor depends upon the thermal microwave emission from water vapor in the atmosphere contrasting with the very low emission from the highly reflective ocean surface. This water vapor emission increases with water vapor content. Two closely spaced frequencies having very different water vapor absorption characteristics allow the unique retrieval of the water vapor information in the presence of other surface and atmospheric variations which do not depend strongly on frequency. Thus, the SSM/I 19.35 and 22.235 GHz channels (22.235 GHz being centered on a water vapor absortion line) can be compared and through physical radiative tranfer models be related to a certain water vapor content of the atmosphere. These retrievals have historically proven to be as close to radiosonde observations as can be expected for two measurment systems with such different spatial averaging characteristics.

### 1.2.2 liquid water

Total liquid water content can be retrieved at the same time as the water vapor. It will present virtually the same TB warming at 19.35 and 22.235 GHz, and the warming at 37 GHz can be used as well, to evaluate through radiative transfer modeling how much cloud water is needed to produce the desired warming. This radiometric signal is particularly strong, producing over $100^{o}$ TB increases over the ocean. However, the amount of liquid water retrieved is very dependent upon what drop size distribution is assumed in the modeling, a few larger drops resulting in more of a signal than many small drops. Thus, it is very difficult at present to confidently partition the TB warming into separate fractions of rain water and cloud water. Our inability to accurately measure these quantities in situ makes algorithm validation particularly difficult. However, since the areal distribution of precipitation is very much smaller than cloud liquid water, we can often assume that the liquid water signal is due entirely to clouds. As the signal becomes very large, some rain must be assumed (because the larger drop sizes of rain produce much greater effects even when the water content is the same) and the degree of partitioning becomes as much an art as it is science. It is hoped that future microwave radiometers will allow spectral separation of the cloud and rain signals with lower frequencies (e.g. 6 and 10 GHz).

### 1.2.3 near-surface oceanic wind speeds

Near surface oceanic wind speeds can be retrieved through the empirical relationship that exists between wind speed and the degree of wind roughening and foam generation on the surface. With SSM/I dual polarization measurements at 37 GHz, the effects of atmospheric water vapor and surface roughening can be separated. Buoy comparisons have revealed standard errors of about 2 m $s^{-1}$ with this method. Unfortunately, if cloud water amounts become too large, not enough of the surface can be seen to get a good surface signal. Thus, wind speeds will not be retrievable with the SSM/I where moderate or greater cloud water amounts are present. This disadvantage of 37 GHz becomes much less at 10 GHz and below. In fact, wind speeds and precipitation rate are now routinely measured during aircraft reconnaisance flights into hurricanes in the 4 to 7 GHz region. Another problem is that small spacecraft attitude changes, if not taken into account, can result in cross-swath biases in wind speed of several meters per second. This has happened with the first SSM/I and empirical correction procedures are being worked out by several investigators.

### 1.2.4 precipitating ice

Ice precipitation, either above rain, or snow falling over water, can be observed at 85.5 GHz through weighted differencing of the vertically and horizontally polarized TB (Spencer et al., 1989). Non-cirrus ice produces TB depressions as soon as the ice is large enough to precipitate. TB

SEPTEMBER 1987 PRECIPITABLE WATER ( mm )

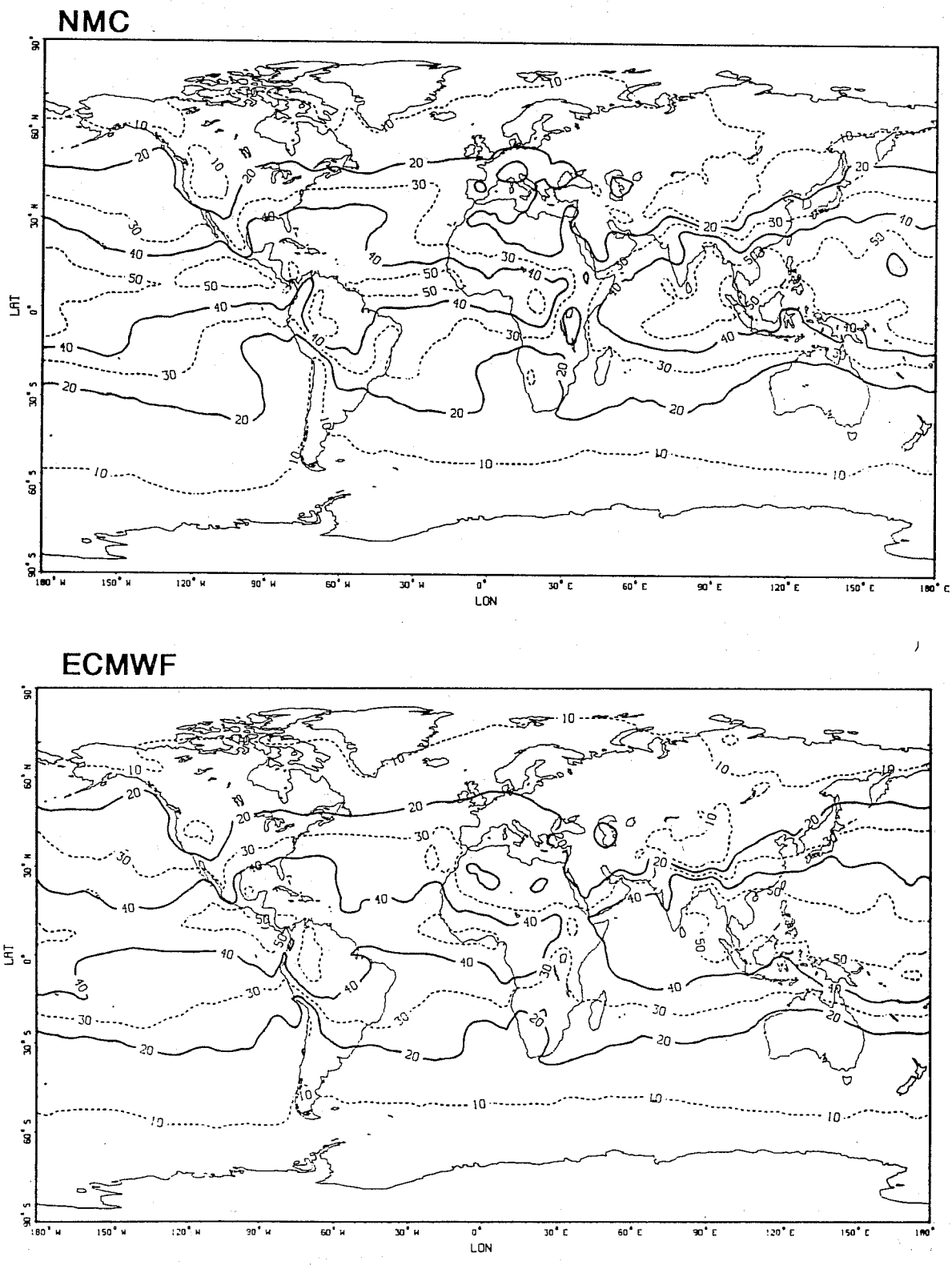


Figure 1. September mean NMC and ECMWF analysis of precipitable water. Note contour interval of 10 mm (equivalent to 1.0 g $cm^{-2}$).

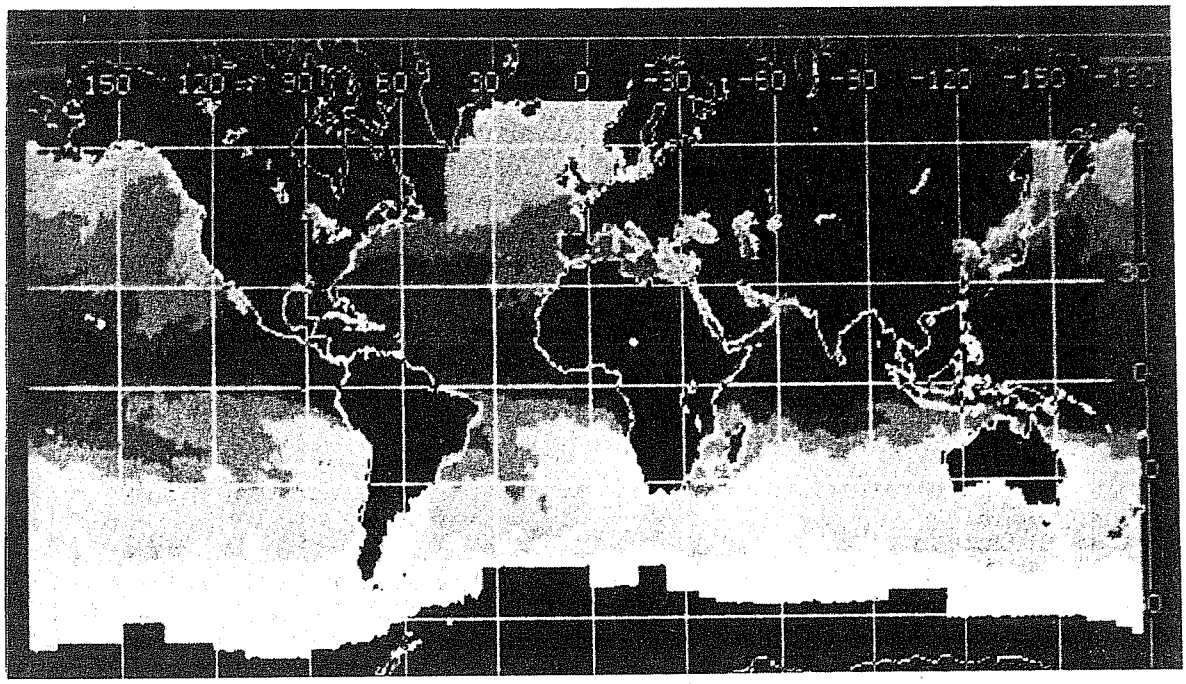


*Figure 2. September 1987 monthly mean precipitable water (g $cm^{-2}$) from SSM/I. Six gray shades (light -> dark) correspond to the following intervals: .0-1.0, 1.0-2.0, 2.0-3.0, 3.0-4.0, 4.0-5.0, >5.0.*

depressions of up to 200° have been observed in intense storms, and very light precipitation of a couple of millimeters per hour can produce ten degree depressions. Unfortunately, some (mostly oceanic) precipitation is not associated with an ice phase, and the lower frequencies (e.g. 19.35 GHz) must be used to observe the thermal emission from the rain (although with the difficulties mentioned above concerning drop size distributions). The ice scattering at 85.5 GHz, though, allows ice precipitation over land to be retrieved as well, where thermal emission by the rain cannot be seen at the lower frequencies due to the similarity of the signal to the radiometrically warm land surface. Ice precipitation can be distinguished from cold land by differencing the 85.5 and 37 GHz TB, which will both be depressed by cold land, but the higher frequency TB will be depressed relatively more by precipitation. While the amount of TB depression appears to be related to variations in precipitation intensity, this relationship probably varies considerably between different climatic regimes. Fortunately, the precipitation area seems to be well correlated with the areas of 85.5 GHz depressions, and this should prove to be a useful validation tool alone.

### 1.2.5 Database and Algorithms

Passive microwave data used in this study were obtained from Remote Sensing Systems, Inc., courtesy of Dr. Frank Wentz. The data include calibrated brightness temperatures and geophysical retrievals from the SSM/I flown aboard the polar-orbiting DMSP satellite. The retrievals used in this study are column-integrated water vapor or precipitable water, W, and column-integrated total liquid water, L (Wentz, 1983). The SSM/I data were navigated and composited in digital image form on the MSFC McIDAS (Man computer Interactive Data Access System). At present only the 1800 Local Equator crossing data swaths for September 1987 have been used. Gridded OLR data from the NOAA polar orbiter 2 archived at 2.5 degree resolution were also composited to form a monthly mean for September 1987. Measured values (no interpolated data) corresponding to the 1430 L Equator crossing were used. The NMC and ECMWF 2.5 degree resolution global gridpoint analyses were used to obtain precipitable water. The OLR data, NMC and ECMWF analyses were obtained from archives at NCAR.

## 2. DIAGNOSTIC RESULTS WITH SSM/I (SEPTEMBER 1987)

This study attempts to bring together microwave and infrared measurements as well as independent global gridpoint analyses in understanding the distribution and structure of atmospheric moisture and clouds over oceanic regions.

### 2.1 Precipitable Water

Because water vapor is by far the largest component of atmospheric moisture it is a quantity of primary interest. Figures 1 and 2 show monthly means of W as depicted by the NMC and ECMWF analyses and as determined from SSM/I, respectively. There are striking quantitative similarities between

the estimates, both showing strong zonal asymmetries, however, the ECMWF analyses tend to have less meridional variability in the oceanic basins. Tropical moisture in the Pacific maximizes west of the dateline and has a constricted latitudinal extent along the west coasts of North and South America. The subtropical minima straddling the Equator in the eastern Pacific are colocated with climatological positions of the subtropical ridges. A similar though less extensive pattern is present over the tropical Atlantic. Regions of strong moisture gradient (e.g. subtropical eastern Atlantic and Pacific, South Indian Ocean) appear well captured by the analyses. SSM/I estimates seem slightly drier, particularly in the deep tropics west of the dateline where they are smaller than NMC amounts by about twenty percent. The source of this disagreement is evidently related to the algorithm in the SSM/I calculation in that areas with some liquid moisture caused W to be a bit drier than actual. A new algorithm is being readied to compensate for these cloudy areas.

Some measure of the moisture variability at the time scale of synoptic transients is obtained from Fig. 3 which shows the standard deviation of daily SSM/I W values with respect to the September monthly mean. Transient activity maximizing east of the continents clearly identifies middle latitude storm tracks. The largest variability exists east of Japan, but significant fluctuations extend across the N Pacific to 150$^{o}$W. The presence of synoptic transients in the South Atlantic and South Pacific convergence zones is also apparent. In the subtropics, variability noted off the west coast of Mexico is consistent with the presence of several tropical cyclones which traversed this region in September. There is a notable lack of variability over moist tropical oceans (e.g. western Pacific and off the west coast of Central America).

**2.2 *Total Liquid Water (TLW) Content***

Because condensation often occurs in convective towers and mesoscale regions, it would be natural to expect TLW exhibit more small scale detail than the environmental water vapor field. This is supported in Fig. 4 which shows the granular nature of the September mean TLW. Narrow concentrations of water along the ITCZ in the Atlantic and eastern Pacific give way to a broad region of liquid water west of the dateline. Visible too are relative maxima along middle latitude storm tracks; these features seem in general to be less organized than the signatures in the W field standard deviations shown in Fig. 3. The standard deviation of TLW (not shown) is very similar in pattern and has values which are consistently larger than the monthly mean. Although the northern hemisphere (NH) storm tracks show more variability in W than do those in the southern hemisphere (SH), the SH TLW appears at least as large as in the NH. Compare for example the north Atlantic storm track with the South Atlantic convergence zone located southeast of Brazil. This may be a result of stronger NH land/sea contrast altering poleward moisture

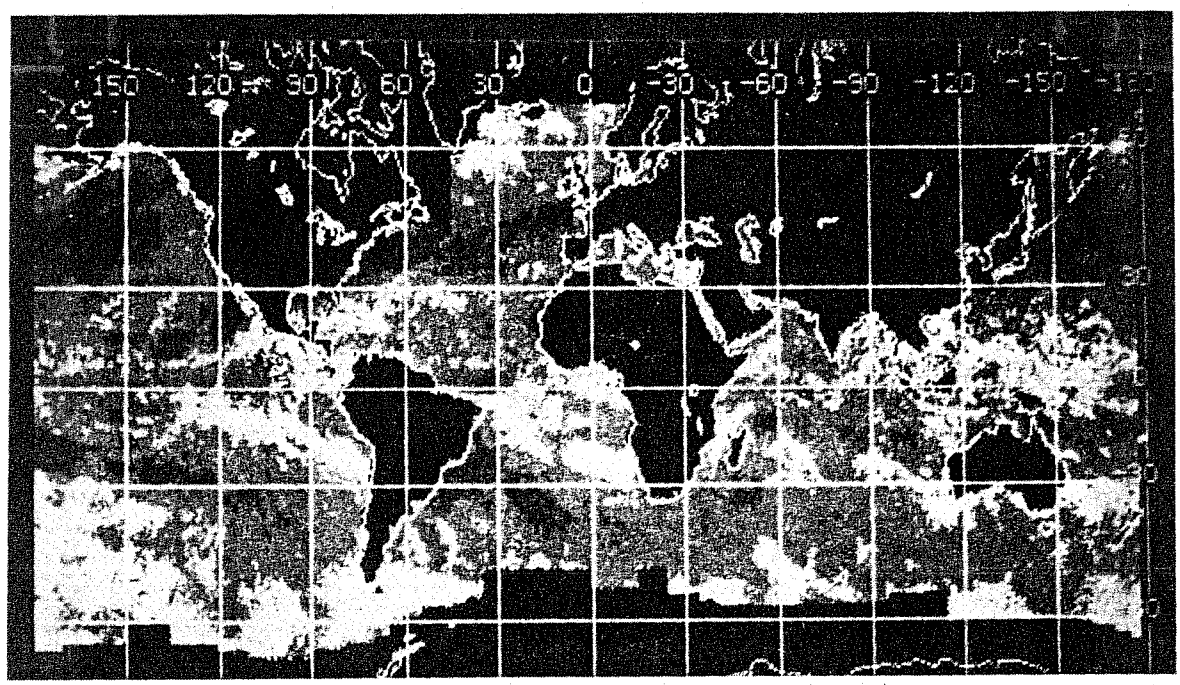

*Figure 3. Standard deviation of monthly mean precipitable water from SSM/I (g $cm^{-2}$). Four gray shades (light -> dark) correspond to the following intervals: .0-.16, .16-.32, .32-.64, .64-1.28.*

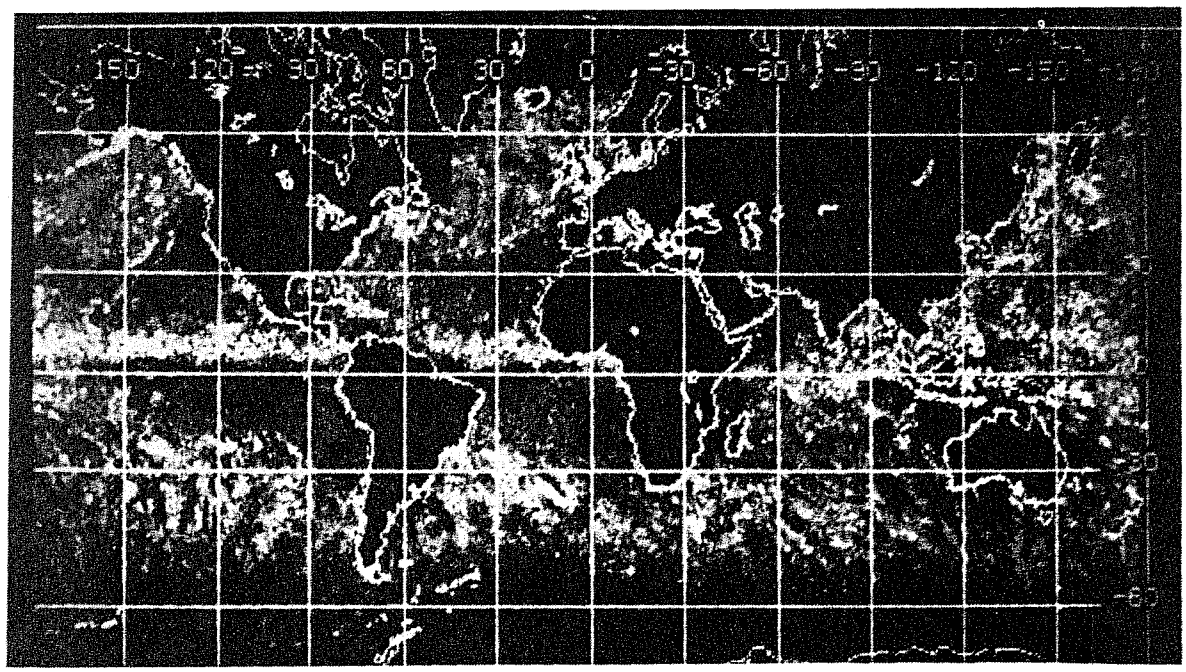

*Figure 4. September 1987 monthly mean total liquid water (mg $cm^{-2}$) from SSM/I. Four gray shades (dark -> light) correspond to the intervals: 0-8, 8-16, 16-32, >32.*

transport and associated precipitation structure.

**2.3 Precipitating Ice**

The distribution of precipitation size ice (or snow covered ground) shows a very distint band along the ITCZ in the western hemisphere. Large areas with little or no indication of precipitation from cold clouds were found in the subtropical oceans, especially in the SH. In the western N Pacific, intense precipitation tracks were associated with individual typhoons during September 1987.

**2.4 Relationship to Other Measurements**

Outgoing Long-wave Radiation (OLR) has traditionally served as a surrogate for the intensity of deep convection and rainfall in the tropics. Because high TLW amounts are associated with precipitation it is useful to compare these quantities. Patterns of TLW in Fig. 4 and September 1987 mean OLR in Fig. 5 show good correspondence in the tropics, at least on this time scale. OLR less than 225 W $m^{-2}$ is generally coincident with high TLW amounts. Poleward of the subtropical ridges, the relationship weakens. Storm tracks in the southern Atlantic and Pacific oceans show that regions of maximum TLW do not necessarily correspond to relative minima in OLR.

SST analyses for September (NMC, Fig. 6) bear a close resemblence to W in the tropics, implying a strong control of atmospheric moisture by SST patterns on this time scale (Neelin and Held, 1987).

**2.5 ECMWF Moisture Flux Divergence**

The vertically integrated moisture flux divergence determined from ECMWF data for September 1987 is shown in Fig. 7. The divergence is partitioned in Fig. 8 into that supplied by the mean flow (top) and the transient eddies (bottom). In the tropical regions it is clear that moisture is removed from the subtropics and deposited in the equatorial latitudes by the mean flow, generally associated with the ITCZ. For this particular month, the Pacific was in the midst of a warm phase of the Southern Oscillation, so that values over the mid Pacific may be greater than normally observed. The moisture is also removed from the subtropics by the eddies which then deposit the water in the midlatitudes. The zero line of divergence in midlatitudes is almost exactly along the axis of greatest standard deviation found in W from SSM/I (Fig. 3).

**2.6 Summary**

A high degree of consistency is exhibited among the SSM/I derived moisture, NMC and ECMWF precipitable water and OLR for the one month period presented. It would seem that to incorporate these SSM/I derived data into initialization schemes for operational analyses would lead to enhanced accuracy of several meteorological parameters, especially over oceanic areas.

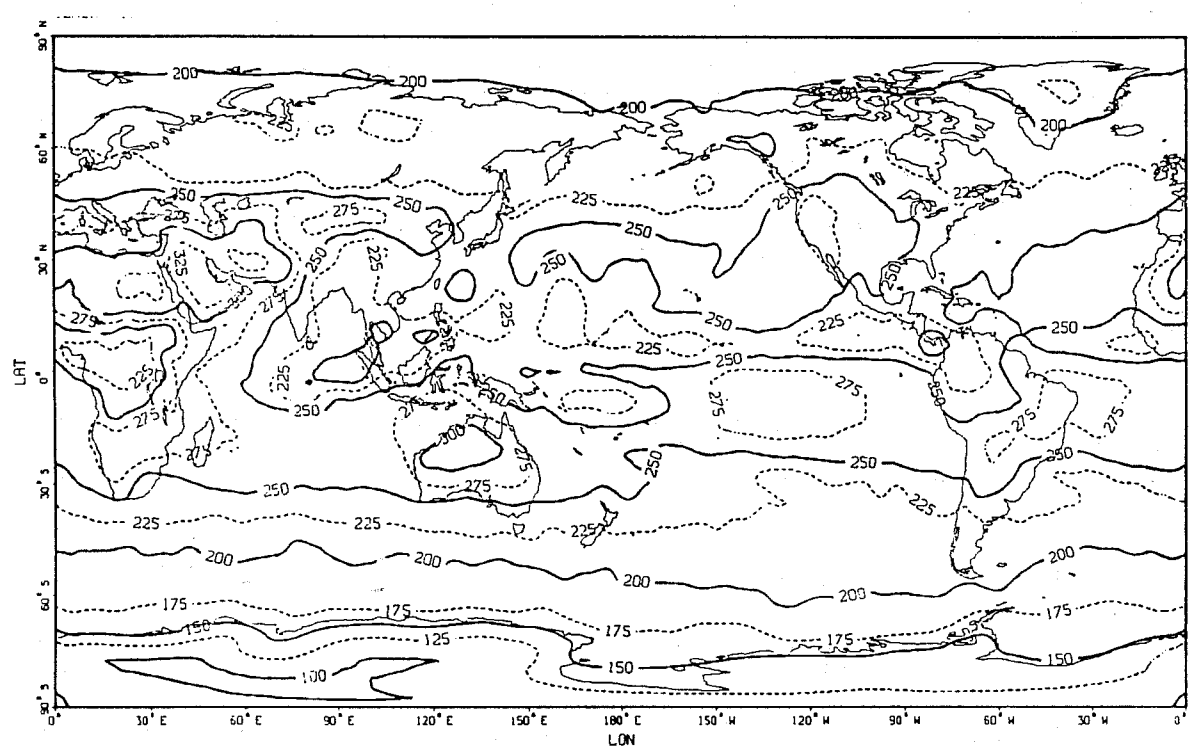


Figure 5. September mean daytime OLR (W $m^{-2}$).

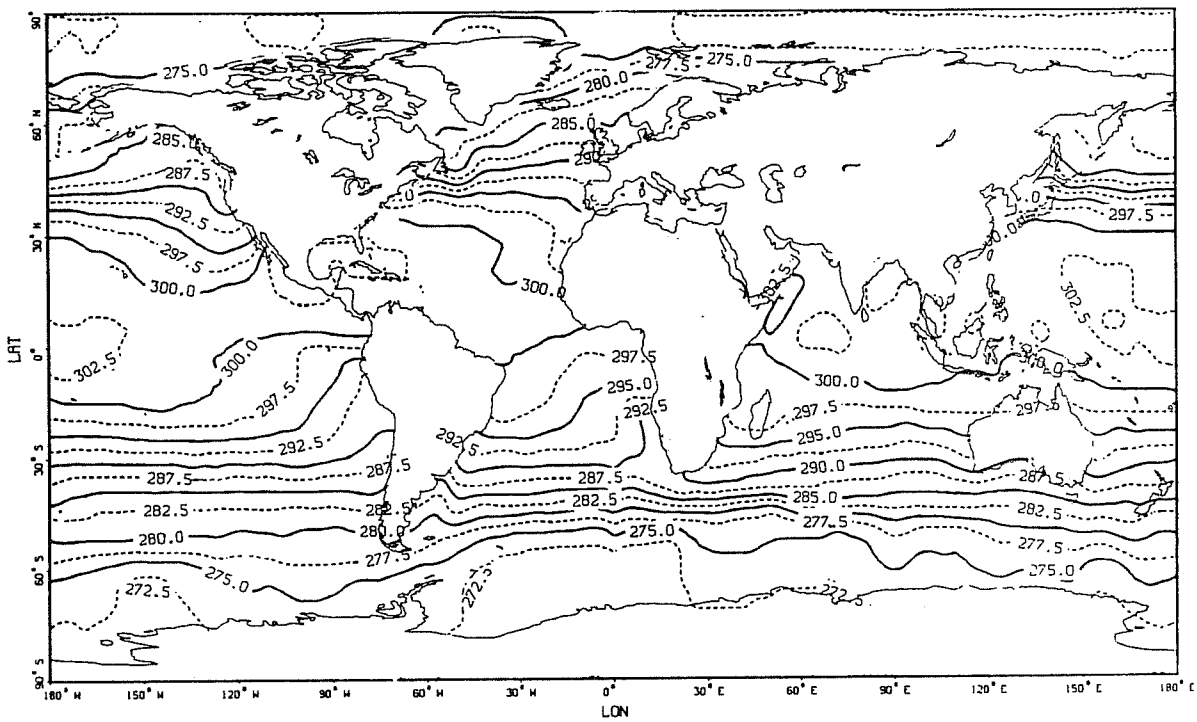


Figure 6. September 1987 mean sea surface temperatures from NMC analyses.

ECMWF - DIAGNOSED EVAPORATION MINUS PRECIPITATION
VERTICALLY-INTEGRATED (mm / day X 10 )

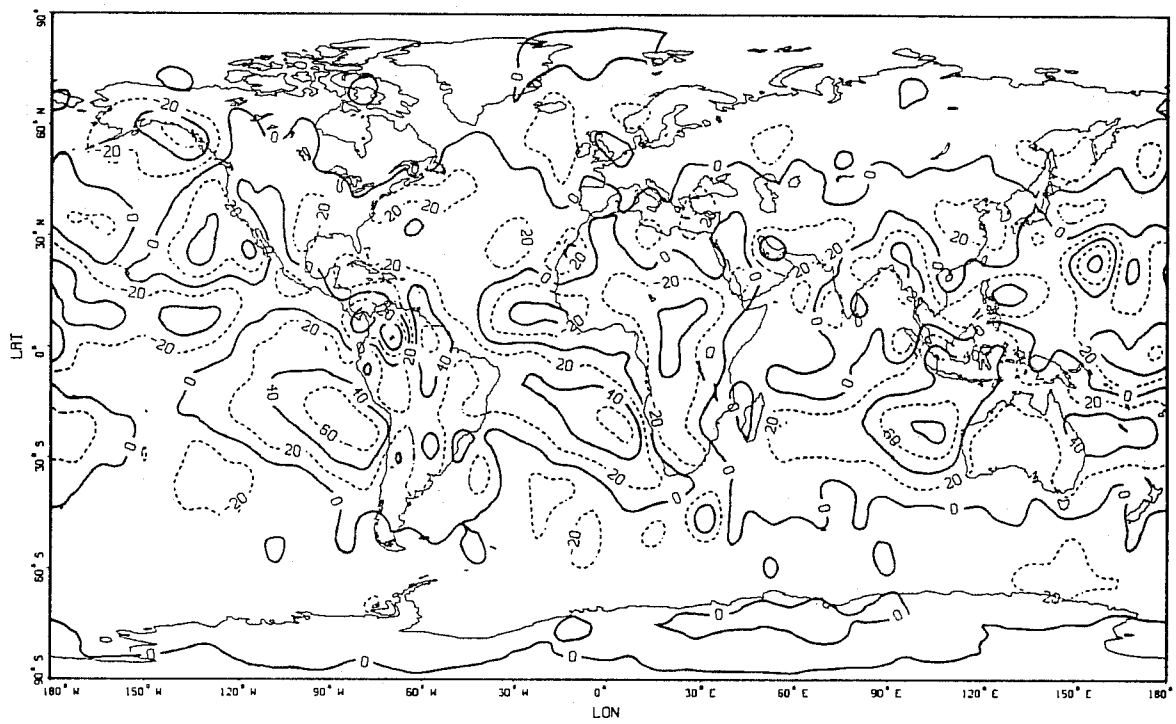


Figure 7. Vertically integrated divergence of the moisture flux from ECMWF analyses for September 1987.

SEPTEMBER 1987 ECMWF VERTICALLY-INTEGRATED MOISTURE DIVERGENCE (MM / DAY X 10 )

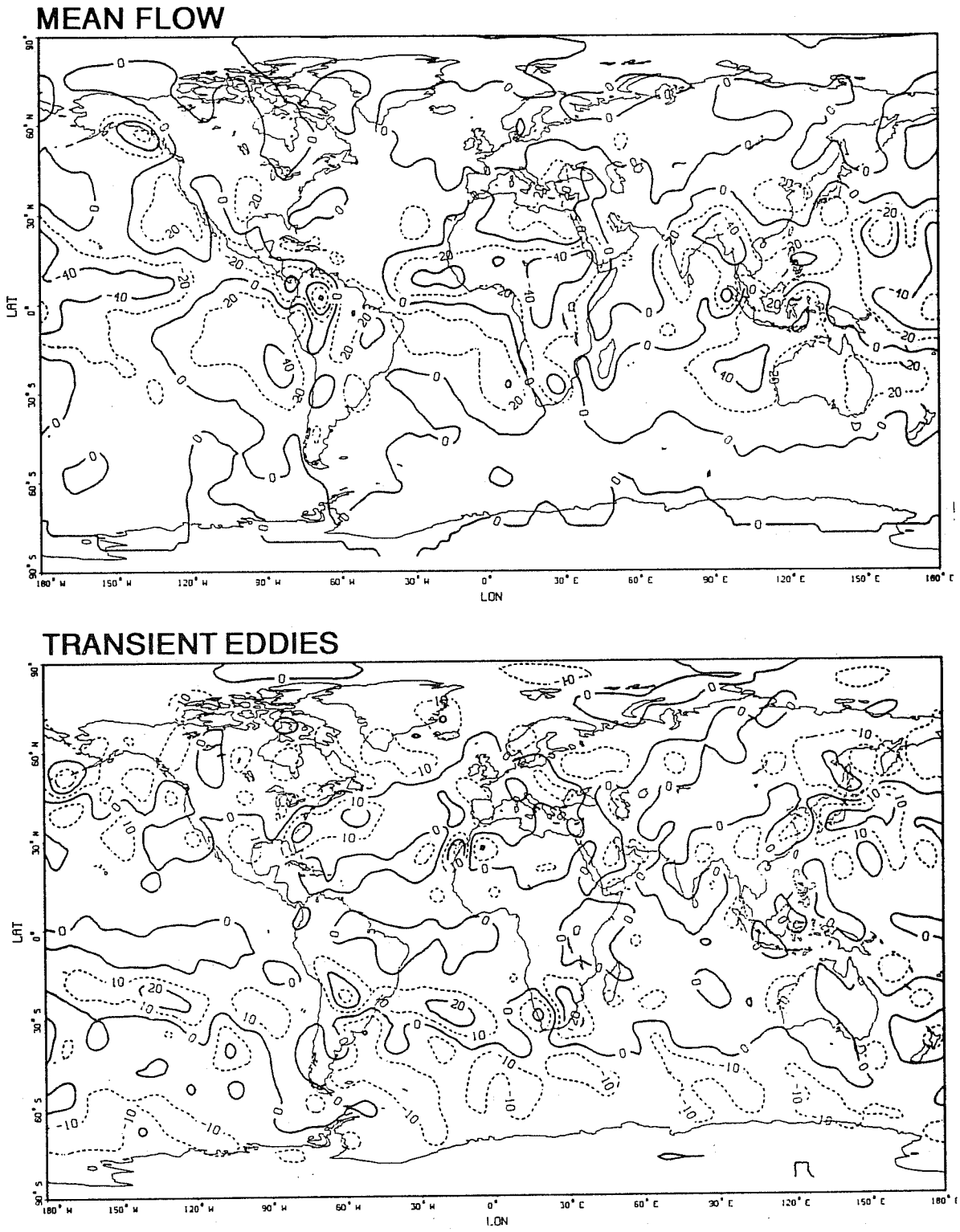


Figure 8. Top: Vertically integrated divergence of the moisture flux due to the mean flow for September 1987. Bottom: as above but for the eddies.

## 3. DIAGNOSTIC ASSIMILATION OF SSM/I DATA

In order to develop an accurate, dynamically consistent description of the atmospheric hydrologic cycle it is desirable ultimately to blend the retrieved SSM/I values with data from other sources. A motivation for doing this is to overcome some weaknesses of each data type. For example, because of the nature of the radiative transfer processes in SSM/I frequencies, little direct information concerning the vertical distribution of measured quantities is retrievable. Furthermore, since the SSM/I flies on a polar orbiting satellite, the data swaths are asynoptic in nature. One possible methodology to alleviate these shortcomings is a diagnostic assimilation of SSM/I products into a global, time-dependent model of the moisture equations. Velocity fields (u,v and $\omega$ ) from the ECMWF analyses (or other global analyses) would be used to drive conservation equations from water substance (e.g. vapor, cloud water, cloud ice, rain and snow). Source and sink terms in these equations would consist of bulk microphysical parameterizations (e.g. Kessler, 1969; Rutledge and Hobbs, 1983). The evolving fields of water substance would then be periodically updated or constrained by SSM/I retrievals. With exception of the SSM/I updating, this concept is in many ways analogous to retrieval of microphysical quantities from multiple Doppler radar wind retrievals. Obviously, the different space scales demand a careful examination of the manner in which microphysical processes are parameterized.

The use of parameterized microphysical equations allows the development of a vertical structure of moisture consistent with the large-scale observed kinematic field. Constraints of these evolving water substance fields can be introduced in an integral sense via SSM/I retrievals. For instance, the time-dependent diagnostic model would supply the shape of the relative humidity profile at a given gridpoint, while the precipitable water would be periodically updated from SSM/I. Similarly, the vertical profiles of the hydrometeor fields can be provided by the model, while constraints on the bulk amounts are periodically supplied from the microwave retrievals. A conceptual diagram of this procedure is shown in Fig. 9.

There are a number of advantages to this approach. First, it provides a means for quantitatively relating the microwave depiction of atmospheric moisture to atmospheric flow fields. Furthermore, this is done in a synoptic framework since the SSM/I data are assimilated using a time-dependent model. This would facilitate studies of synoptic scale systems. Analyses of cloud and precipitation fields to land areas would also be possible, although updating of fields would be limited to ice since emission-based algorithms work only over water.

Several crucial issues must be resolved to make this procedure effective. First, there is the accuracy of the archived

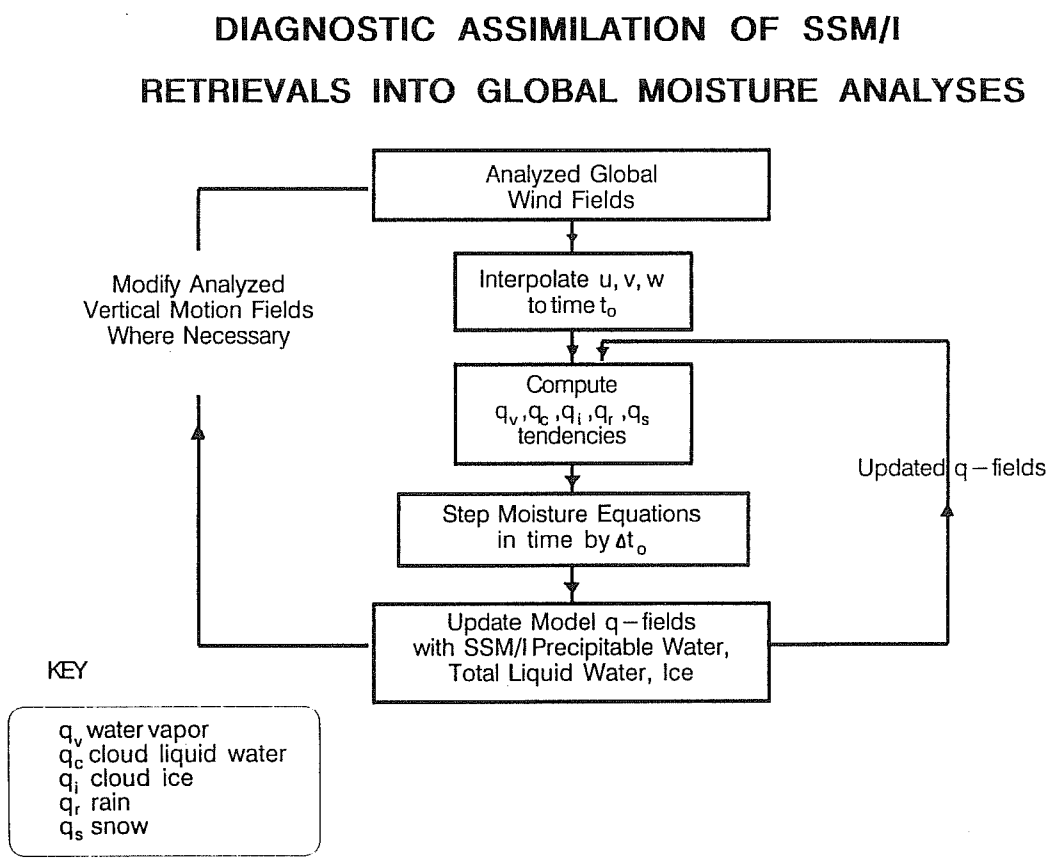


Figure 9. Conceptual diagram of assimilation process using SSM/I retrievals to constrain moisture and condensate predicted using global u,v,$\omega$ wind analyses.

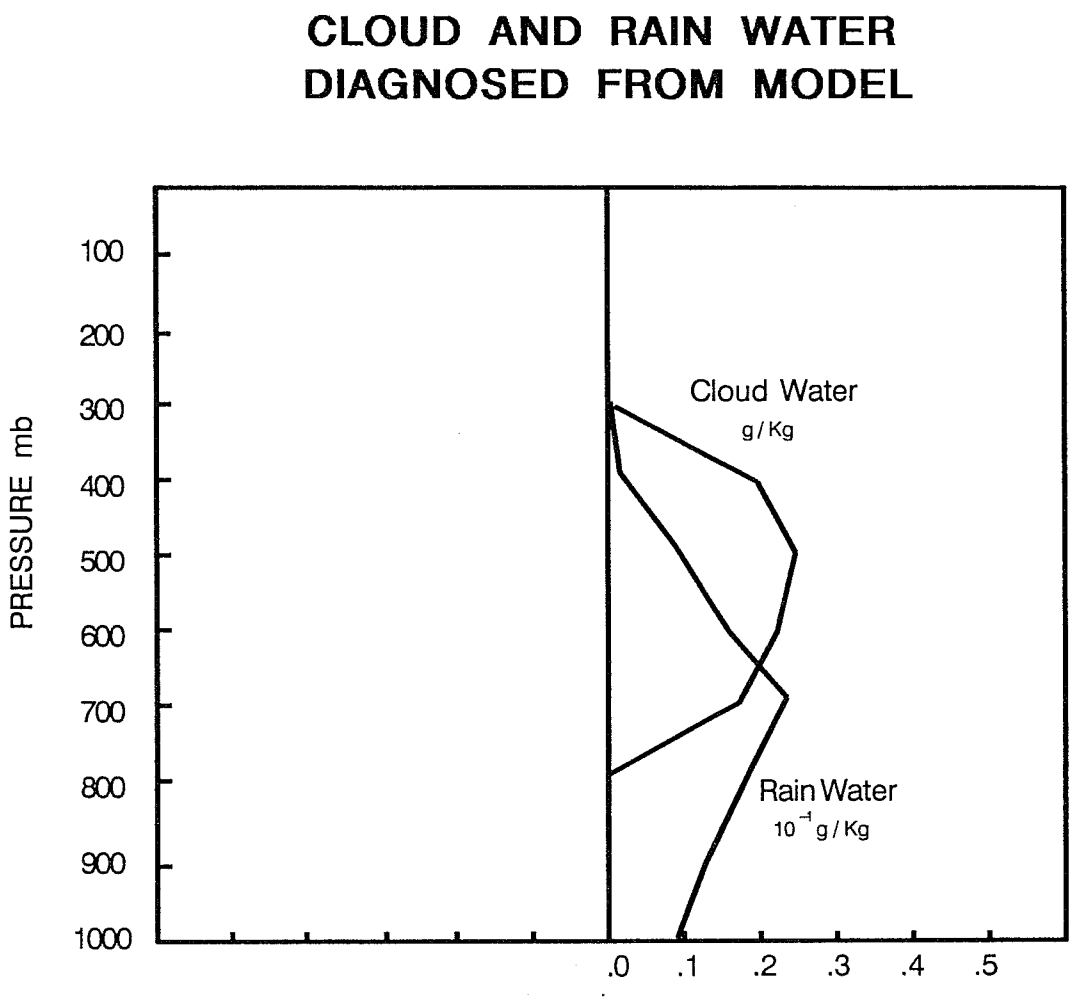


Figure 10. Vertical profile of cloud and rain water determined from a 1-D model which was initialized with ECMWF temperature, vertical motion and humidity data. Location corresponds to a developing storm in the North Atlantic on 1 September 1987.

vertical motions which exert a strong constraint on the moisture and condensate fields. Gross errors in magnitude as well as phase are likely over data poor regions such as oceans. Some modification of these fields may be necessary based on the SSM/I retrieved bulk quantities. Some treatment of fractional cloudiness will also be necessary since the SSM/I footprint sizes are substantially smaller than the archived global wind analyses. Related to the fractional cloudiness problem is the treatment of convection, both deep and shallow. The former requires a parameterized updraft to detrain moist air and condensate to the grid-scale. Parameterized shallow convection in the diagnostic model is necessary to treat extensive marine stratocumulus. Because this cloudiness is likely to exist in regions of downward grid-scale motion, a representation based on surface moisture fluxes is likely to be required.

The microphysical formulation for a diagnostic assimilation model is currently being developed. Figure 10 shows a vertical profile of cloud and rainwater diagnosed using a one-dimensional model. Profiles of vertical motion, temperature and water vapor have been taken from the ECMWF analyses at 1200 UTC 1 September 1987. The sounding is located in a developing storm system in the North Atlantic. A more complete model treating ice processes is being completed now.

## 4. ACKNOWLEDGEMENTS

The authors extend thanks to Dr. Frank Wentz, Remote Sensing Systems, for supplying the SSM/I radiances and derived products. This research is supported by the NASA Global Scale Atmospheric Processes Research Program, Dr. Ramesh Kakar, Program Manager; and by the Mesoscale Processes Research Program, Dr. James Dodge, Program Manager.

## 5. REFERENCES

Kessler, E., III, 1969: On the Distribution and Continuity of Water Substance in Atmospheric Circulations, Meteor. Monogr., No. 32, Amer. Meteor. Soc., 84 pp.

Neelin, J. D. and I. M. Held, 1987: Modeling tropical convergence based on the moist static energy budget. Mon. Wea. Rev.,115, 3-12.

Rutledge, S. A. and P. V. Hobbs, 1983: The mesoscale and microscale structure and organization of clouds and precipitation in midlatitude cyclones. Part VIII. J. Atmos. Sci., 40, 1185-1206.

Spencer, R. W., H. M. Goodman and R. E. Hood, 1989: Precipitation retrieval over land and ocean with the SSM/I, Part 1: Identification and characteristics of the scattering signal. J. Atmos. Oceanic Tech., submitted.

Wentz, F. J., 1983: A model function for ocean microwave brightness temperatures. J. Geophys. Res.,88, 1892-1908.